2013 IEEE International Conference on Robotics and Automation (ICRA)
Karlsruhe, Germany, May 6-10, 2013

Fault Detection Algorithm for External Thread Fastening by Robotic Manipulator Using Linear Support Vector Machine Classifier

Takayuki Matsuno[1], Jian Huang[2] and Toshio Fukuda[3]

***Abstract*— Fault detection functions with learning method of a robotic manipulator are very useful for factory automation. All production has the possibility to fail due to unexpected accidents. To reduce the fatigue of human workers, small errors automatically should be corrected by a robot system. Also a learning method is important for fault detection, because labor of system integrator should be reduced. In this paper, an external thread fastening task by a robotic manipulator is investigated. To discriminate the four states of a task, linear support vector machine methods with two feature parameters are introduced. The effectiveness of the proposed algorithm is confirmed through an experiment and recognition examination. Finally, the ability of linear SVM is compared with artificial neural network method.**

I. INTRODUCTION

Fault detection functions [1][2] are very useful for factory automation. Difficult assembly tasks [3] which are currently conducted by human workers have the possibility of failing. To avoid stopping production lines, workers should observe robots engaged in assembly tasks and should eliminate the causes of unexpected small accidents which happen occasionally. To reduce the tasks and fatigue of workers, such small errors should automatically be corrected by a robot system. In this paper, an external thread fastening task by a robotic manipulator is investigated. Almost all home electrical appliances consist of both plastics components and electrical circuits. An electrical circuit has to be screwed to a plastics component. Therefore, external thread fastening tasks are necessary in current production lines. Here, an external thread and a screw make same exterior appearance. But, it is assumed that the female hole for a thread (a screw) has already been scraped out in this research. Therefore, we define the fastener component as "an external thread" in this paper.

Some studies on thread fastening tasks have been reported. Klingajay et al. [4] proposed an on-line estimation method of parameters such as the screw diameter and friction for a tapping task. Mrad et al. [5] proposed a fuzzy logic control method of both the screw driver and the xyz-table to avoid process failures. A visual servo is also useful for automation of the screw fastening task [6]. A mechanical disassembly tool to loosen a screw was also proposed by Zuo et al. [7]. The purpose of their research was to make an automation system for the disassembly of home electrical appliances.

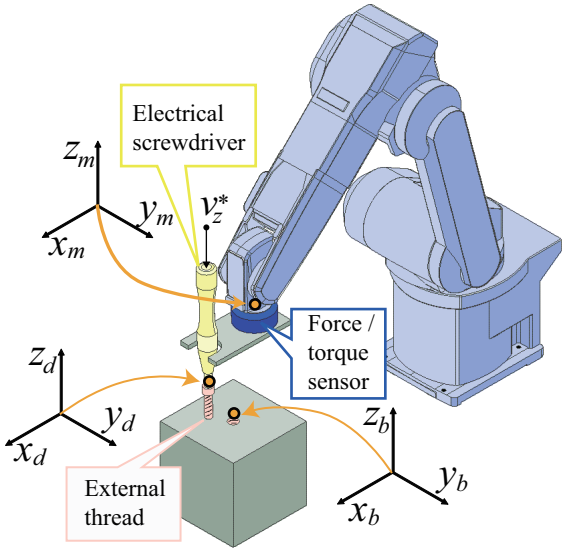

Fig. 1. Robot system configuration for thread fastening task

However, in current production lines, only the simple fault detection method of measuring the torque increase signals of a screwdriver is applied. Although specialized machines currently do thread fastening tasks, in this paper, a robotized assembly process is assumed. Under this assumption, to avoid collisions and damage, a robot manipulator has to have a force/torque sensor on its wrist and achieve compliance control in contact tasks, as shown in Fig. 1. By analysis of the motion of a thread in a hole, it was found that vibration synchronized with the angular velocity of the screwdriver always occurs when a robot fastens a thread. By measuring this vibration from the force sensor data, the inserted length of a thread can be estimated. We have already proposed fault detection method for external thread fastening [8].

In this research, four states of a screw fastening task are defined, as shown in Fig. 2. A successful state is illustrated in Fig. 2(a). After realizing this state, a robot can continue on to the next task. An empty state, in which the robot accidentally misses a screw, is illustrated in Fig. 2(b). When this state occurs, the robot gets an external thread from the station and tries to fasten the thread again. A failed state, in which the robot misaligns the external thread in the threaded hole, is illustrated in Fig. 2(c). Finally, a jammed state, in which

[1]T. Matsuno is with Graduate School of Natural Science and Technology, Okayama University, 3-1-1 Tsushima-naka kita-ku, Okayama, Okayama, 700-8530, JAPAN matsuno@cc.okayama-u.ac.jp

[2]J. Huang is with the Department of Control Science and Engineering, Huazhong University of Science and Technology, Wuhan 430074, CHINA huang_jan@mail.hust.edu.cn

[3]T. Fukuda is with the Department of Micro-Nano Systems Engineering, Nagoya University, Furo-cho-1, Chikusaku, Nagoya, Aichi, 464-8603, JAPAN fukuda@mein.nagoya-u.ac.jp

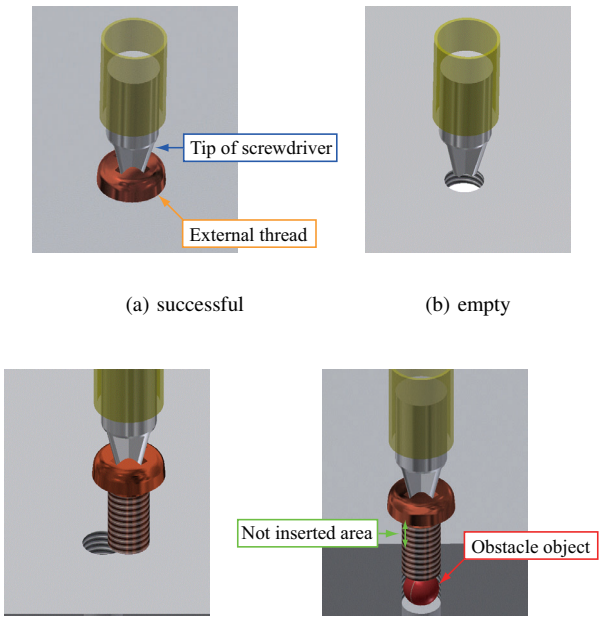

(a) successful (b) empty

(c) failed (d) jammed

Fig. 2. External thread fastening task states

an unnecessary object impedes the process of insertion, is illustrated in Fig. 2(d). In this state, the robot must pull out the screw and fasten a new thread.

Our research purpose is to discriminate these four task states by using a linear support vector machine (linear SVM) [9] with two feature parameters. One parameter is the estimated insertion length. This parameter can be calculated by observing the vibration of the torque measured by the force sensor on the robot wrist. In this paper, we explain the reason why this vibration phenomenon occurs during an external thread fastening task. The motion of a male thread coupled with a female thread was analyzed by Hagiwara et al. [10]. However, the thread, named the X-screw, was specified for a power transmission. In our research, the motion of a commonly used external thread which is fastened into a threaded hole is analyzed. Also, The second feature parameter is the maximum reaction force. The effectiveness of the proposed algorithm is confirmed through an experiment and an examination. Finally, the ability of linear SVM is compared with artificial neural network method.

II. THREAD FASTENING EXPERIMENT

In this section, the experimental condition is described first. Second, the force and position data for the successful state and each error state are presented. Finally, the difficulty of estimating the state is discussed.

A. Experimental Condition

In this subsection, the experimental condition is described. As shown in Fig. 1, a force sensor is fixed on the wrist of the robot manipulator, and an electrical screwdriver is fixed on the other side of the force sensor. Here, the "m" coordinate system is set as the sensor frame, and the "d" coordinate system is set as the frame of end-effector. It is on the tip of an electric screwdriver. Also, the "b" coordinate system is set as the base frame. The origin of the base frame is on the top and center of thethreaded hole. The directions of "m" and "d" coordinate system are consistent with that of "b" coordinate system in an initial instant of fastening task. The robot manipulator is controlled with compliance control based on the force sensor information. The sampling time of force feedback is approximately 7 ms. The center of compliance control is set on origin of "d" frame. With this control, the robot manipulator has compliance in the x_b-, y_b-, z_b-axis directions and no compliance for the x_b-, y_b-, z_b-axis rotations. The manipulator has compliance in the x_by_b-plane because it has to adjust the position of the external thread over the center of the hole. Also, the manipulator has compliance in the z_b direction to avoid damaging both the external thread and the threaded hole from the excessive force generated by position control with high precision. Then, the desired position of the end-effector moves in the vertical direction with velocity v_z^*. The other desired positions are kept initial values during fastening task. The v_z^* can be calculated with equation (1).

$$v_z^* = \alpha_z l_p \frac{\omega_d}{2\pi}. \tag{1}$$

Here, l_p indicates the pitch of the external thread, and α_z, which is set at 1.03, is the coefficient of velocity. The angular velocity of screwdriver ω_d must be known because we use this parameter in the algorithm to calculate a feature parameter. The angular velocity is always 14 π [rad/s] (7 [rps]) in this experiment.

Photos of the tip of the screwdriver during thread fastening are shown in Fig. 3. We use a CLF-7000 (HIOS Corp.), which is an electric screwdriver with a suction air line for the vacuum apparatus. A thread is picked up and fixed on the tip of the screwdriver by the vacuum force. The size of the external thread is M5 $\times$ 12 mm, and its pitch is 0.8 mm. The material is stainless steel. The threaded hole has enough depth for the external thread. Also, the screwdriver can generate sufficient torque to maintain the angular velocity against friction during the task to fasten the external thread. Finally, we set the conditions to stop the thread fastening task, as follows.

1) In the case that the position of the end-effector gets to the end point.
2) In the case that the measured reaction force exceeds threshold F_{zmax}.

In this paper, F_{zmax} is set at 50 [N], and the end point for the end-effector is set at the lowest position where the tip of the electric screwdriver does not collide against the base plate under the condition without the external thread on the tip.

B. Experimental Result

Thread fastening experiments are conducted under the condition that each state occurs intentionally. In this paper,

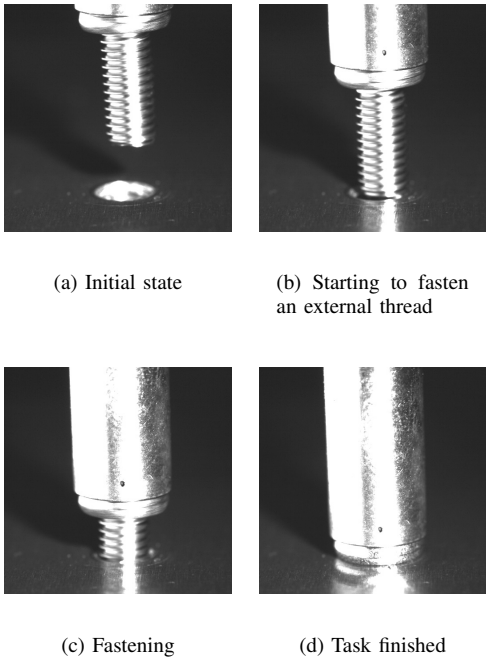

(a) Initial state (b) Starting to fasten an external thread

(c) Fastening (d) Task finished

Fig. 3. Photos of external thread fastening

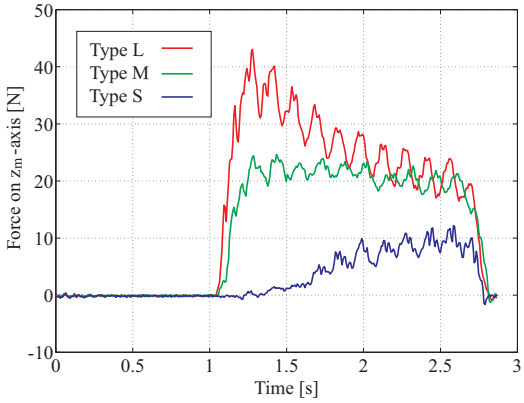

Fig. 4. Measured reaction force on z_m-axis in the successful state

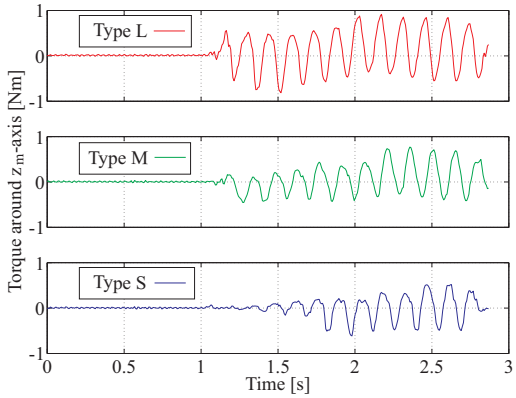

Fig. 5. Measured reaction torque around the z_m-axis in the successful state

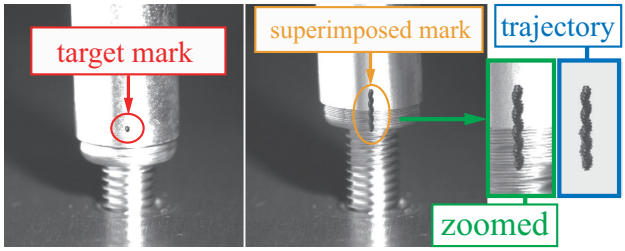

Fig. 6. Trajectory of the tip of the screwdriver on the $y_b z_b$-plane captured by high speed camera

experiments are conducted 50 times for each state to obtain data.

The experimental data are shown in Fig. 4 to Fig. 8. The reaction force measured by the force sensor is plotted in Fig. 4. Successful states are grouped according to their maximum values into three types: S (small), M (medium) and L (large). The different reaction forces, Types S, M and L, were generated because of the phase differences between the movement of the end-effector going down and the rotation of the electric screwdriver.

In the case that the phase coincides well, the initial reaction force is small, as in Type S. In the out-of-phase cases, as in Types M and L, the reaction force becomes bigger at the instance of contact. In every case, the contact of the external thread begins at approximately 1.0 second. If the phase completely coincides, the reaction force does not occur. However, in this paper, the reaction force conveys important information for the fault detection algorithm. Therefore, to obtain the reaction force in spite of the phase difference, the velocity of the desired position is forced to be fast by α_z in equation (1). The measured reaction torques around the z_m-axis are shown in Fig. 5. It should be mentioned that the vibration of the reaction torque is synchronized with the rotation of the electric screwdriver in each force type. We explain the reason why such vibration of measured torque occurs in Section III. A part of trajectory of the tip of the screwdriver on the $y_b z_b$-plane is shown in Fig. 6. The trajectory is ploted by superimposing a target mark on tip of screwdriver captured by a high speed camera with 250 fps. As explained above, compliance control with force sensor information is adopted. Therefore, those trajectory vibrates by force from the head of the thread. However, because the magnitude of the force rapidly changes, compliance control cannot completely cancel the force from the head of the thread due to the delay of the force feedback. Although the start points of the trajectories are the same, the goal points of the trajectories differ, because the connection between the head of the external thread and the tip of screwdriver is not fixed firmly. Therefore, their relative position may go out of alignment.

Next, the measured reaction forces in the three error states are plotted in Fig. 7. In the empty state, the reaction force does not occur. In the failed state and the jammed state, the

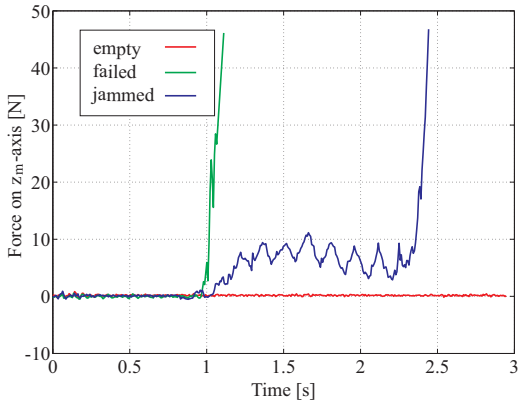

Fig. 7. Measured reaction force on the z_m-axis in the three error states

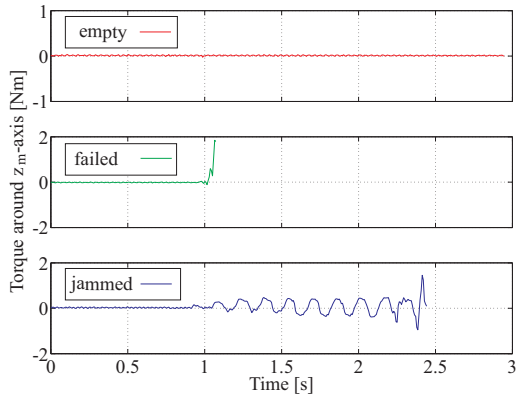

Fig. 8. Measured reaction torque around the z_m-axis in the three error states

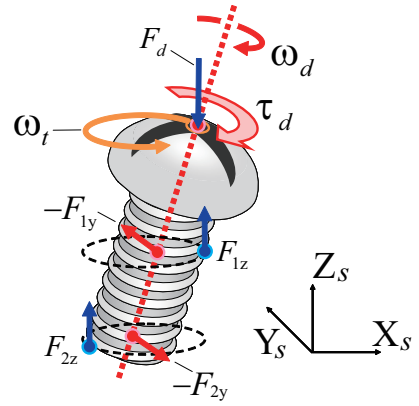

Fig. 9. Force and torque acting on the external thread

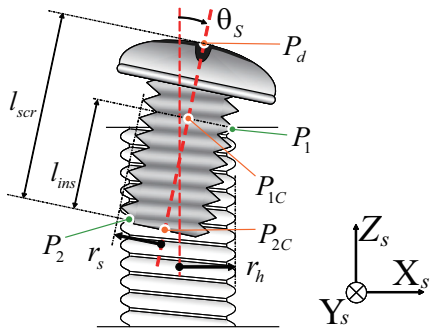

Fig. 10. Configuration of the external thread in the internal thread hole

reaction force reaches the threshold F_{zmax} and the task is finished. Finally, the measured reaction torques in the three error states are plotted in Fig. 8. It is known that slight vibration of the reaction torque occurs at the instance of contact despite the failed state, in which an external thread is not inserted.

C. Difficulty of Fault Detection and Diagnosis

In a general assembly task, the insertion work time and the inserted length can be calculated easily with threshold processing for the measured reaction force. However, it is difficut for a threshold processing method to distinguish between the success state and the error states. As shown in Fig. 4, the difference of the phase of the screw determines the maximum value of the reaction force, even if they belong to the success state. Therefore, another method is required for discrimination of the four states in the thread fastening task.

III. VIBRATION PHENOMENON IN THE THREAD FASTENING TASK

In this section, the reason is explained for the vibration occurring in the robotized thread fastening task in the above-mentioned experiment. This vibration phenomenon occurs only under the condition that a robotic manipulator fastens an external thread with an electrical screwdriver.

A. Configuration of Screw Fastening

In this subsection, the configuration of the thread fastening action and the parameters are described. First, as shown in Fig. 9, let us consider the situation that the external thread contacts two points of the threaded hole. We define the plane which goes through the two contact points and is parallel to the vertical direction as the xz plane of the "s" coordinate system. Then, the posture of the external thread in the threaded hole becomes as shown in Fig. 10. The external thread with respect to the industry standard has a smaller diameter than that of the threaded hole. Therefore, when an external thread is directed down by the tip of screwdriver, it inclines with an angle of θ_s [rad], as shown in Fig. 10. The parameters are defined in Table I.

B. Quasi-static Analysis of Thread Fastening

In this section, the generation of the vibration synchronized with the rotation of screwdriver is explained. Before thread fastening, the external thread is secured on the tip of the screwdriver by a vacuum and rotates with the screwdriver. Here, an electric screwdriver has sufficient torque τ_d to maintain the angular velocity ω_d. Let us consider the situation that the head of the external thread is directed down by force F_d.

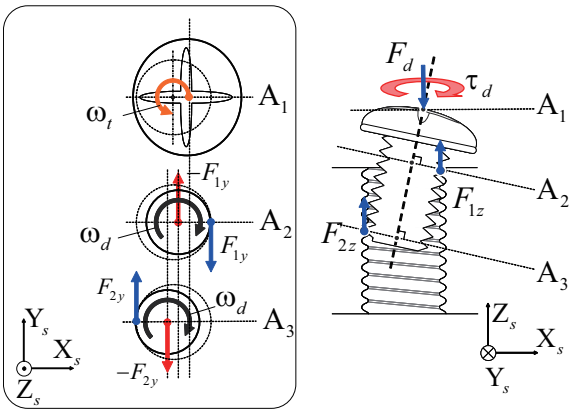

Fig. 11. Screw and the threaded hole

TABLE I

PARAMETERS FOR THE MODEL OF EXTERNAL THREAD DYNAMICS

Parameter	Meaning	Unit
F_d	Force vector from screwdriver to a screw.	[N]
F_1	Force from threaded hole on P_1. the elements are $[F_{1x}\ F_{1y}\ F_{1z}]^T$.	[N]
F_2	Force from threaded hole on P_2. The elements are $[F_{2x}\ F_{2y}\ F_{2z}]^T$.	[N]
l_{scr}	Whole length of external thread.	[m]
l_{ins}	Inserted length of external thread.	[m]
P_1	Upper contact point between external thread and hole.	
P_2	Lower contact point between external thread and hole.	
P_{1C}	The cross point between center line of external thread and vertical plane passing through P_1.	
P_{2C}	The cross point between center line of external thread and vertical plane passing P_2.	
P_d	Contact point between thread and screwdriver	
r_s	Radius of external thread.	[m]
r_h	Radius of threaded hole.	[m]
τ_d	Driving torque to fasten an external thread generated from screwdriver.	[Nm]
ω_d	Angular velocity of rotation motion of external thread.	[rad/s]
ω_t	Angular velocity of orbital motion of external thread.	[rad/s]

First, two contact points exist between the external thread and the threaded hole. We define the point on the upper side as P_1, and that on lower side as P_2. Then, the reaction forces F_{1z} and F_{2z} on P_1 and P_2, respectively, are calculated as

$$F_{1z} = \frac{r_h + \epsilon}{2r_h} F_d, \tag{2}$$

$$F_{2z} = \frac{r_h - \epsilon}{2r_h} F_d. \tag{3}$$

Here,

$$\epsilon = \left(l_{scr} - \frac{l_{ins}}{2} \right) \sin\theta_s. \tag{4}$$

We assume that the contact condition keeps the stick state without slip on each point in this paper. With this assumption, friction force F_{1y} and F_{2y} are generated on each contact point P_1, P_2, respectively, as shown in Fig. 11. When the friction force is less than the maximum static frictional force, the stick state is maintained and

$$F_{1y} = \frac{\tau_d}{2r_s} < \mu F_{1z}, \tag{5}$$

$$F_{2y} = \frac{\tau_d}{2r_s} < \mu F_{2z}. \tag{6}$$

Here, μ is the coeffient of maximum static friction between the external thread and the threaded hole. F_{1y} and F_{2y} are the same magnitude, but the direction is opposite. P_{1c} is a cross point between the center line of the external thread and the perpendicular line that goes down from P_1 at the center line. Likewise, P_{2c} is a cross point for P_2. Because the fastening torque does not affect a point on the center line, $-F_{1y}$ and $-F_{2y}$ are dominant forces. In the case that an external thread is inclined for a hole, $-F_{1y}$ and $-F_{2y}$ are the moments of a couple. As a result, this moment of a couple around the center line is an orbital motion. With the assumption of the stick state of the contact points, the angular velocity of orbital motion ω_t is calculated by equation (7).

$$\omega_t = \frac{r_s \cos\theta_s}{r_h} \omega_d. \tag{7}$$

The rotation motion of the center line of the external thread appears as a rotation motion of P_d, which is the contact point between the tip of the screwdriver and the head of the external thread. The force sensor on the wrist of the manipulator robot, which is controlled with compliance motion control, measures the vibration of the torque data synchronized with the rotation of the screwdriver. According to tolerance specification of threads, $0.08[mm] < r_h - r_s < 0.15[mm]$ can be calculated in this experimental condition. Therefore, there is an enough clearance gap where screwdriver can move on the $x_b y_b$-plane even if inclination of an external thread became zero. Actually, an external thread slackened as far as we can turn around it, in the case fastening of thread is not completed.

Next, we consider the situation of the slip state on the contact points. When F_d is not zero, the friction forces $\mu' F_{1z}$ and $\mu' F_{2z}$ affect P_{1c} and P_{2c}, respectively. Here, μ' is the coefficient of dynamic friction on the contact points. In this situation, because the moment of inertia of the external thread is sufficiently small, a large angular acceleration instantaneously occurs. Then, the angular acceleration generates the rotation motion of the external thread. It is believed that as a result, the contact condition soon shifts from the slip state to the stick state.

C. Discussion

In this section, we explain the friction resistance that affects the points on the center line of the fastener thread. Because the two points of application of the friction resistance are out of alignment due to the thread inclination, motion of the center line of the external thread is generated. When a worker fastens a thread, he/she tries to reduce the friction force as much as possible. Also, the angular velocity

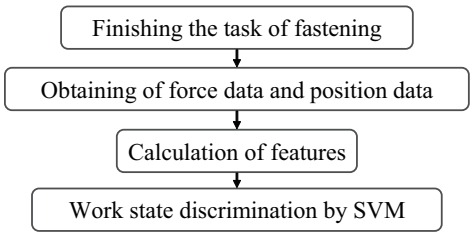

Fig. 12. Scheme of fault detection

during fastening is not constant. Therefore, the vibration phenomenon is unique to robotized thread fastening.

IV. FAULT DETECTION BY THE SUPPORT VECTOR MACHINE

The learning method for fault detection is useful in the sense that some parameters necessary for discrimination are automatically obtained from the learning data. In this paper, the linear SVM with the sequential minimal optimization (SMO) method is adopted for fault detection and fault diagnosis. In this section, state discrimination using the linear SVM is explained. First, the scheme of fault detection is described. Next, two features of the SVM are introduced. Finally, the result of the recognition rate examination is described.

A. Scheme of Fault Detection

As shown in Fig 12, our fault detection algorithm consists of three parts. Because all the data is required for calculation of the feature parameters, the robot starts the fault detection algorithm after a finished task.

A linear SVM classifier is made for the combination of each state. In this paper, a total of six linear SVM classifiers are made by the combination of the four states. In the process of classifying, the success state and the other error states are compared in series by the SVM classifier, as shown Fig. 13. Once an error state is found in this process, the combination of error states are compared by the SVM classifier.

B. Feature Parameters of the SVM

Here, the two feature parameters of the linear SVM are introduced for fault detection. One is the estimated insertion length and the other is the maximum reaction force.

First, the estimated insertion length is explained. The estimated insertion length is calculated by counting the number of waves of vibration caused by the thread fastening. Here, C_{corr}, the autocorrelation coefficient of the torque around the z$_m$-axis M_z in the separated interval Δt, is calculated as shown in Fig. 14. Δt is expressed by equation (8).

$$\Delta t = \frac{1}{2}\frac{2\pi}{\omega_d} = \frac{\pi}{\omega_d}\ [\text{sec}]. \tag{8}$$

Fundamentally, Δt is the half cycle of the rotation motion of the thread head. It should be the half cycle of ω_t. However, it is difficult to calculate ω_t accurately, because ω_t is a time-varying function with some arguments as shown in equation (7). Therefore, as $\omega_t \approx \omega_d$, the half cycle of ω_d is used for

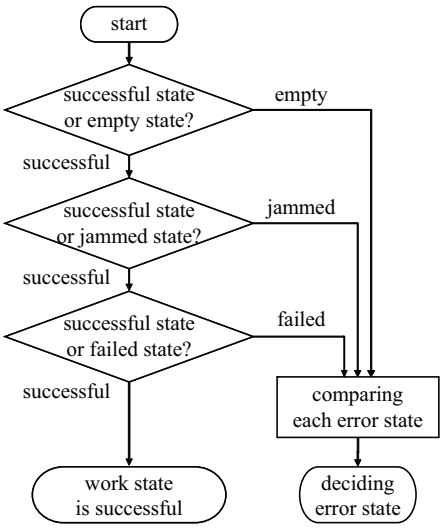

Fig. 13. Application process of the SVM

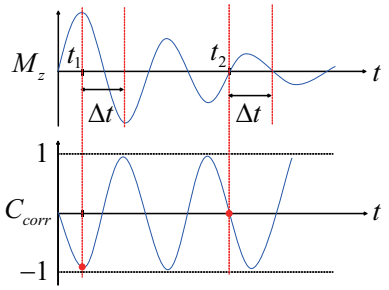

Fig. 14. Calculation example of the coefficient of autocorrelation

calculation. By calculation of C_{corr}, two effects are expected. One is that we can obtain normalized data from -1.0 to 1.0, regardless of the magnitude of the original torque data. The other is that unnecessary higher-frequency noise data is cut off. Figure 15 shows C_{corr} for the torque data in Fig. 5. It is clear that, despite the magnitude of the torque, the coefficient of autocorrelation can be obtained in each type. Also, Fig. 16 shows C_{corr} for the torque data in Fig. 8. It is known that vibration noise cannot generate a clear waveform in the coefficient of autocorrelation. Thus, N_{zc} is defined as the effective count of the zero crosses of C_{corr}. Here, "effective count" means the check of the condition of the waveform of C_{corr} from one cross point to the next cross point. The conditions checked are listed below.

1) Intervals of the cross points should be within the margin of error of plus or minus 10% Δt.
2) The maximum absolute value of C_{corr} in the neighboring cross points should be higher than criterion C^*_{corr}.

In this research, C^*_{corr} is set at 0.5. If one waveform satisfies both of these conditions, N_{zc} is counted. After the counting of N_{zc}, the estimated insertion length $\hat{l}_{ins}$ is calculated by

$$\hat{l}_{ins} = \frac{N_{zc} lp}{2}. \tag{9}$$

The second feature parameter is the maximum reaction

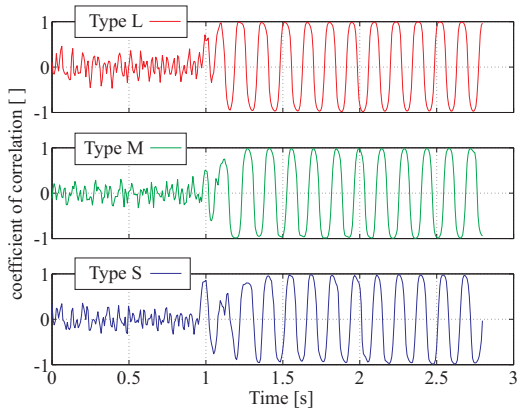

Fig. 15. Calculated coefficient of autocorrelation of the reaction torque around the z_m-axis

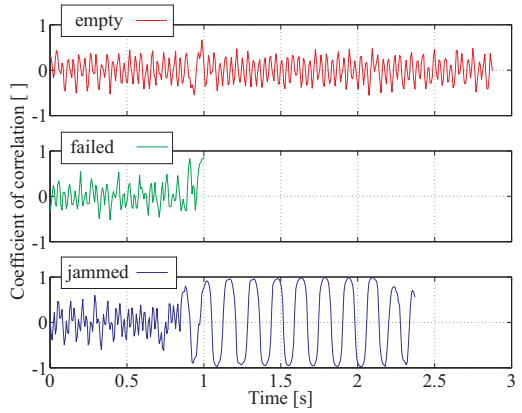

Fig. 16. Calculated coefficient of autocorrelation of the reaction torque around the z_m-axis for the empty, jammed and failed states

force. Because of the measuring error, even if we adopt the abovementioned algorithm, $\hat{l}_{ins}$ is sometimes calculated as a non-zero value in the empty state. To simplify the discrimination of the empty state in the linear SVM classifier, the maximum reaction force is introduced.

C. Condition for Discrimination Examination

In this subsection, conditions for the discrimination examination are described. Here, 50 data are obtained for each state. The 25 data in the jammed state are obtained with a hole depth of 5.4 mm, and the other 25 are obtained with a hole depth of 8.6 mm. In each state, 25 data are randomly selected as learning data of the SVM. The other 25 data for each state are used as evaluation data. To calculate the average of the SVM recognition rate, the abovementioned examination is conducted 10 times.

D. Discrimination Result of the SVM

The average recognition rate result over 10 examinations is shown in Table II. A row of the table expresses the task state of the evaluation data, and a column expresses the recognition result. As shown, we achieve a high recognition rate of over 90%. However, in the fourth row of the first column, the cell is 0.4%, which is a problem. This means that

TABLE II
RECOGNITION RATE OF THE SVM FOR THE THREAD FASTENING TASK (10 TIMES)

Evaluation data	Recognition rate [%]			
	Successful	Empty	Failed	Jammed
Successful state	99.6	0	0	0.4
Empty state	0	100	0	0
Failed state	0	0.8	98.0	1.2
Jammed state	0.4	0	2.4	97.2

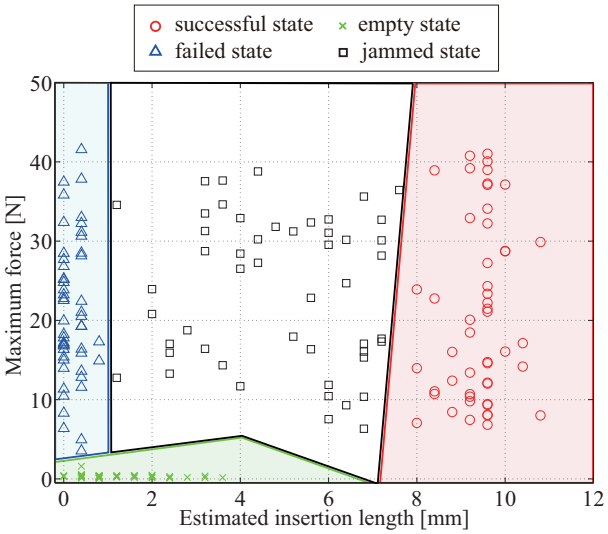

Fig. 17. Feature parameters for the SVM discrimination

in this case, it is possible that the jammed state is recognized as a successful state by the SVM classifier. Therefore, in a production line, the fault detection system will overlook a defective product. Improvement of the recognition rate is one of our future tasks.

Next, all of the feature parameters are shown in Fig. 17. Here, the horizontal axis is the estimated insertion length, and the vertical axis is the maximum reaction force. Also, the recognition results of the SVM, where all of the recognitions are correct, are plotted. The polylines of the linear discriminant generated by the SVM classifier. It is clear that polylines of discrimination are drawn to separate four state.

V. ARTIFICIAL NEURAL NETWORK

Here, we compare linear SVM classifier with artificial neural neural (ANN) in discrimination of task states. We use hierarchical artificial neural network with normalized sigmoid function as shown in Fig.18, and adopt a back propagation method for learning.

The average recognition rate result over 10 examinations is shown in Table III. There is no meaningful difference with SVM in recognition ability. Next, the outpur of ANN and feature parameters are shown in Fig. 19. However, it takes too long time to learn stable output with ANN. The itereration number and average of output error is shown in Fig. 20. The back propagation should be conducted two thousand times,

TABLE III

RECOGNITION RATE OF THE ANN FOR THE THREAD FASTENING TASK (10 TIMES)

Evaluation data	Recognition rate [%]			
	Successful	Empty	Failed	Jammed
Successful state	98.6	0	0	1.4
Empty state	0	99.6	0	0.4
Failed state	0	0.8	99.8	0.2
Jammed state	0	0	5.2	94.8

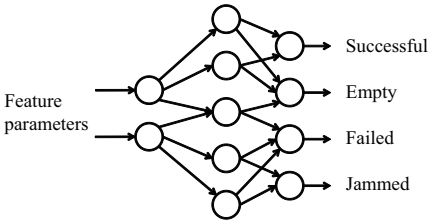

Fig. 18. Configuration of ANN

and it takes about 40 seconds with PC which has core2Duo 1.33GHz CPU. On the other hand, it takes about 5 seconds to optimize linear SVM classifier with same conditions.

Therefore, linear SVM classifier is better than ANN method in the sense of calculation cost, when the map of feature parameters is simple like our case. It should be confirmed that classifier is required to discriminate more complicated map. It is one future work.

VI. CONCLUSION

Fault detection functions of a robotic manipulator are very useful for factory automation. In this paper, a thread fastening task by a robotic manipulator was investigated. The method to estimate the inserted length of a thread from vibration of the measured torque is proposed. To discriminate the four states of the fastening task, the linear SVM classifier was introduced with two feature parameters. One is the estimated insertion length, and the other is the maximum reaction force. The effectiveness of proposed algorithm was confirmed through an experiment and a recognition examination. The average recognition rate for 10 examinations was over 90%. Finally linear SVM classifier is compared with ANN method. Linear SVM classifier is better than ANN method in the sense of calculation cost, although discrimination abilities are approximately same.

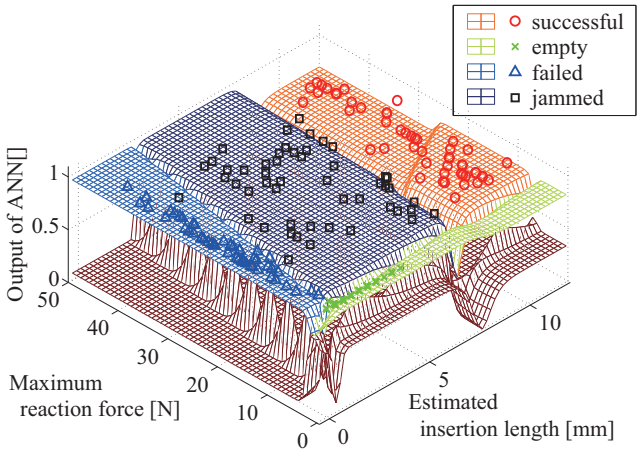

Fig. 19. Feature parameters on ANN discrimination

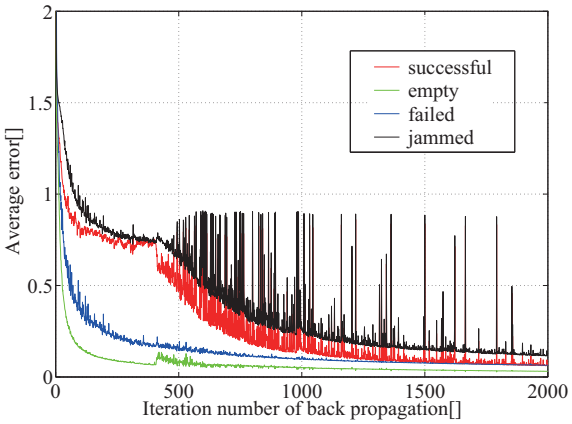

Fig. 20. Output error in ANN back propagation

REFERENCES

[1] J. Huang, T. Fukuda, T. Matsuno, *Model-Based Intelligent Fault Detection and Diagnosis for Mating Electric Connectors in Robotic Wiring Harness Assembly Systems*, IEEE/ASME Transactions on Mechatronics, Vol. 13 Issue 1, pp. 86-94, 2008.

[2] J. Huang, P. Di, T.Fukuda, T. Matsuno, *Robust Model-based Online Fault Detection for Mating Process of Electric Connectors in Robotic Wiring Harness Assembly Systems*, IEEE Transactions on Control Systems Technology, Vol. 18 Issue 5, pp.1207-1215, 2010.

[3] T. Matsuno, T. Fukuda, Y. Hasegawa, *Insertion of Long Peg into Tandem Shallow Hole Using Search Trajectory Generation without Force Feedback*, Proc. of IEEE 2004 International Conference on Robotics and Automation ,Vol 2, pp.1123-1128, 2004.

[4] M. Klingajay, L. D. Seneviratne, K. Althoefer *Identification of threaded fastening parameters using the Newton Raphson Method* Proc. of 2003 IEEE/RSJ International Conference on Intelligent Robots ans Systems, pp.2055-2060, 2003.

[5] F. Mrad, Z. Gao, N. Dhayagude, *Fuzzy logic control of automated screw fastening* Proc. of 1995 Thirtieth Industry Applications Conference Annual Meeting, pp.1673-1680, 1995.

[6] S. Pitipong, P. Pornjit, P. Watcharin, *An automated four-DOF robot screw fastening using visual servo* Proc. of 2010 IEEE/SICE International Symposium on System Integration, pp.379-385, 2010.

[7] Bing-Ran Zuo, A. Stenzel, G. Seliger, *Flexible handling in disassembly with screwnail indentation* Proc. of 2000 International Conference on Robotics and Automation Vol.4, pp.3681-3686, 2000.

[8] T. Matsuno, K. Shiratsuchi, J. Huang, T. Fukuda, *Fault Detection for Thread Fastening by Robotics Manipulator*, Journal of the Robotics Society of Japan (in Japanese), Vol. 30, No. 8, pp. 60-68, 2012.

[9] N. Cristianini, J. Shawe-Taylor, *An introduction to support vector machines and other kernel-based learning* Cambridge University Press, 2000.

[10] T. Hagiwara, S. Hirose, *Development of Dual Mode X-screw -A Novel Load-Sensitive Linear Actuator with a Wide Transmission Range-* Journal of Robotics and Mechatronics, Vol.12, No.2 pp. 66-71, 2000.